

# Evaluation of Image Quality during Upper Abdomen Imaging with Golden-Angle Radial Sparse Parallel-Volumetric Interpolated Breath-hold Examination in Combination with Electromagnetic Wave Suppression Sheet: A Study Using Phantoms

Golden-Angle Radial Sparse Parallel-Volumetric Interpolated Breath-hold Examination と 電磁波抑制シートの併用による上腹部撮像の画質評価:ファントムを用いた検討

ITO Kazuyuki\*, SHIRATO Takashi, YOKOYAMA Hikaru, HAMASAKI Nozomi

Department of Radiology, Juntendo University Nerima Hospital

**Key words:** Golden Angle Radial Sparse Parallel (GRASP), electromagnetic wave suppression, streak artifact, image uniformity

### [Abstract]

**Purpose:** In the context of upper abdominal imaging using Golden-Angle Radial Sparse Parallel-Volumetric Interpolated Breath-hold Examination (GRASP-VIBE), streaking artifacts caused by drooping arms lead to a degradation in image quality. This study examined the effect of employing an electromagnetic wave suppression (EWS) sheet to cover the arm, aiming to reduce streaking artifacts and assess its impact on image quality using a phantom model.

**Methods:** The phantom was arranged to simulate conditions of both raised and lowered arms, and imaging was performed using both GRASP-VIBE and conventional VIBE techniques. The phantom was covered with an EWS sheet, and the streaking artifacts were quantified. Image uniformity was assessed through a gray scale uniformity map.

**Results:** The use of the EWS sheet resulted in a significant reduction of streaking artifacts; however, a notable decrease in uniformity was observed in GRASP-VIBE imaging.

**Conclusion:** The application of the EWS sheet in GRASP-VIBE imaging, when covering the drooping arm, may alleviate streaking artifacts in upper abdominal imaging. Nevertheless, due to radial sampling, signal intensity may fluctuate within the field of view as a consequence of the static magnetic field inhomogeneity induced by the EWS sheet.

### 【要旨】

**目的:**GRASP-VIBE(Golden-Angle Radial Sparse Parallel-Volumetric Interpolated Breath-hold Examination)による上腹部撮像において、下垂した腕から生じるストリーキングアーチファクトは画質劣化の原因となる。本研究では、腕を電磁波抑制(EWS)シートで覆うことによるストリーキングアーチファクトの低減効果と画質への影響を、ファントムを用いて検討した。

**方法**: 腕を上げた状態と下げた状態を想定してファントムを配置し、GRASP-VIBEと従来のVIBEを用いて撮像を行った。腕を模擬したファントムにEWSシートの使用の有無でストリーキングアーチファクトの評価を行った。また画像の均一性をグレースケールマップを用いて評価した。

結果: EWSシートの使用によりストリーキングアーチファクトは有意に減少したが、GRASP-VIBEでは均一性の顕著な低下が観察された.

結論: GRASP-VIBEでの撮像時に下垂した腕をEWSシートで覆うことにより、上腹部撮像におけるストリーキングアーチファクトを軽減できる可能性がある。しかし、ラジアルサンプリングを使用するGRASP-VIBEでは、EWSシートによって誘導される静磁場の不均一性の結果として、FOV内で信号強度の変動を示す可能性がある。

# Introduction

The standard protocol for magnetic resonance imaging (MRI) of the upper abdomen requires patients to suspend respiration during the

伊藤 憲之\*, 白戸 貴志, 横山 光, 濵﨑 望

順天堂大学医学部附属練馬病院放射線科

\* E-mail: kito@juntendo.ac.jp

Received October 31, 2024; accepted January 17, 2025

examination. However, respiratory capacity varies among individuals, and prolonged imaging may result in respiratory artifacts due to inadequate breath-holding. Furthermore, typical respiratory durations (10-15 seconds) impose limitations on spatial resolution and imaging range. Golden-Angle Radial Sparse Parallel-Volumetric Interpolated Breath-hold Examination (GRASP-VIBE) <sup>1)</sup>, a recently developed technique by Siemens, employs a

radial k-space trajectory with golden angles and compressed sensing. GRASP-VIBE demonstrates the capability to acquire images with high temporal and spatial resolution under free-breathing conditions, which can be utilized in dynamic contrast-enhanced (DCE) MRI. The clinical efficacy of this technique has been substantiated in numerous cases <sup>2, 3)</sup>. In our hospital, GRASP-VIBE stands out as the most commonly employed radial imaging methodology for upper abdominal MRI examinations, representing a sophisticated approach in this field. One drawback of GRASP-VIBE is the presence of streaking artifacts inherent to radial imaging 4). While many streaking artifacts in radial images can be attributed to undersampling, the Nyquist condition is violated in the outer regions of k-space. It has also been reported that imaging objects with a large field of view (FOV) causes streaking artifacts due to nonlinearities in the magnetic field gradient at the edge of the magnet 5). Strong streaking artifacts degrade image quality and, in some cases, obscure pathology. In abdominal imaging, a common source of streaks is drooping arms 6. For patients with limited arm mobility due to intravenous cannulation or restricted joint range of motion, imaging is typically performed with the arms positioned inferiorly. The resultant streaking artifacts on the image, caused by the lowered arm position, may potentially compromise the visualization of abdominal organs. Although increasing the number of spokes filling k-space can mitigate streaking artifacts, it also extends the duration of the imaging process.

Currently, there exist medical devices designed to mitigate the effects of electromagnetic waves emitted during MRI examinations. These electromagnetic wave suppression (EWS) sheets are believed to improve image quality by reducing signals that contribute to aliasing and motion artifacts <sup>7)</sup>. However, no studies have yet assessed the image quality of radial

sampling in conjunction with EWS sheets. Our hypothesis posited the possibility of diminishing streaking artifacts through the application of the EWS sheet on the arms during GRASP-VIBE imaging.

The objective of this research was to examine the influence of the EWS sheet on the arms of the images obtained during an upper abdominal examination using GRASP-VIBE by employing phantoms for imaging purposes.

# Materials and Methods

All examinations were performed using a 3T MAGNETOM Vida MR scanner (Siemens Healthcare, Erlangen, Germany) with a BM Spine 32 ch coil and a BM Body 18 ch coil. A spherical phantom (MARCOL-Oil + 0.011 g MACROLEX blue, φ 240 mm, T<sub>1</sub> value 180 ms, T2 value 83 ms) and cylindrical phantoms (NiCl<sub>2</sub>\*H<sub>2</sub>O, H<sub>2</sub>O,  $\phi$  80 mm × 350 mm, T<sub>1</sub> value 57 ms, T2 value 30 ms) that had been used for maintenance of our MRI systems were used as subjects. For the EWS sheet (tranduction sheet ® J·Trust, Tokyo, Japan), 50 cm × 60 cm in size, was used. The EWS sheet comprises copper, acting as an electromagnetic wave reflector, and carbon, serving as an absorber. This sheet is a multilayer structure consisting of copper and carbon, with the exterior of the sheet being copper. Objects covered with this sheet are immune to electromagnetic waves. The sheet is thin and lightweight, making it suitable for wrapping around limbs. The study employed seven distinct phantom configurations, as illustrated in Fig. 1. The phantom diameter was determined by referencing the distribution of abdominal circumference within the Japanese population 8), as published by the Ministry of Health, Labor and Welfare. A spherical phantom with a diameter of 240 mm acted as the torso substitute, while a cylindrical phantom with a diameter of 80 mm served as the arms' representative. The setup featuring two cylindrical phantoms assumed both arms

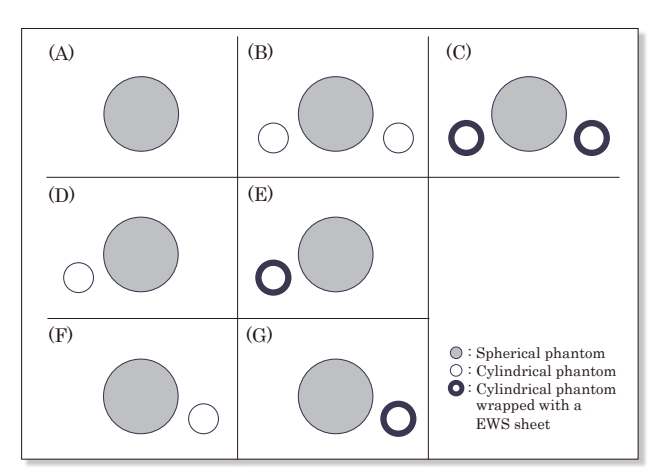


Fig. 1 Schematic representation of the seven phantom configurations.

(A) Central spherical phantom.
(B) Cylindrical phantoms placed on both sides of the spherical phantom.
(C) Configuration B with sheets wrapped around the cylindrical phantoms.
(D) Cylindrical phantom placed only on the right side of the spherical phantom.
(E) Configuration D with a sheet wrapped around the cylindrical phantom.
(F) Cylindrical phantom placed only on the left side of the spherical phantom.
(G) Configuration

F with a sheet wrapped around the cylindrical phantom.

were hanging down, whereas the setup with only one cylindrical phantom assumed one arm was raised. The phantoms were placed at the radiofrequency (RF) coils' center. After allowing the fluid in the phantom to settle for roughly 10 minutes, scanning was performed. In each phantom configuration, imaging was done in the axial section, with the center of the scanning range positioned at the center of the spherical phantom. A single imaging was conducted for each phantom configuration. From the acquired images, the image of the largest cross section of the spherical phantom was chosen for evaluation.

In this research, we employed both GRASP-VIBE and conventional VIBE methodologies. In GRASP-VIBE, the number of radial spokes filling the k-space is contingent upon factors such as duration time, temporal resolution, repetition time (TR), and the utilization of liver gating technique <sup>9)</sup>. To perform GRASP-VIBE, it is necessary to establish the conditions of 2-4 phases. For each phase, a specific duration time is designated, and data is collected continuously for the entire duration

period. Images are then reconstructed using the corresponding number of spokes based on the temporal resolution from the data gathered during the designated duration time. A longer duration time results in more data being collected, leading to a longer scan time. Conversely, increasing the temporal resolution setting increases the number of radial spokes filling the k-space, but diminishes the temporal resolution. The temporal resolution is also influenced by the TR. When employing the self-navigation method of "liver gate," which is a respiratory synchronization technique, only 50% of the data collected on the expiratory side is utilized for image reconstruction. This equates to half the number of radial spokes in the k-space compared to the set temporal resolution. A reduction in the number of radial spokes in the k-space results in an increased influence of streaking artifacts. Respiratory synchronization utilizing the liver gate is essential for imaging the upper abdomen, and it is crucial to control the streaking artifact. Consequently, the experiments conducted in this study were performed under the liver DCE-MRI examination conditions with a combined liver gate employed at our institution. GRASP-VIBE sequence was acquired with the following parameters: FOV  $370 \times 370$  mm, base resolution 288, slice thickness 3.0 mm, slice resolution 68%, slices per slab 72, slice oversampling 11.1%, phase oversampling 0%, TR 3.5 ms, echo time (TE) 1.39 ms, flip angle (FA) 8°, fast fat saturation, slice partial fourier 5 / 8, bandwidth 1160 Hz / Px, Normalize Prescan, phases 4, first duration 15 s, second duration 35 s, third duration 60 s, fourth duration 120 s, temporal resolution 14.6 s, liver gate, delay after bolus 25 s, total acquisition time 4 min 14 s. All analyses were performed using 1st phase images. Conventional VIBE is performed using Cartesian k-space trajectories. Therefore, it was acquired to evaluate the effect of image uniformity resulting from different k-space trajectories. Parameters of conventional VIBE sequence were as follows: FOV 370 × 370 mm, matrix 288 × 288, slice thickness 4.0 mm, slice resolution 61%, slices per slab 60, slice oversampling 20.0%, phase oversampling 10%, TR 3.3 ms, TE 1.15 ms, FA 10°, fast fat saturation, acceleration mode CAIPIRINHA, acceleration factor PE 1, acceleration factor 3D 3, slice partial fourier 7 / 8, bandwidth 620 Hz / Px, Normalize Prescan, total acquisition time 19 s.

# Evaluation of streaking artifacts

We employed a technique to quantify background signal values to evaluate streaking artifacts 4). In areas where signal values are expected to be nearly zero, streaks substantially elevate the average signal. The signal value increases progressively with the intensity of the streaks and approaches zero in their absence. The phantom was imaged using GRASP-VIBE in the configurations illustrated in Fig. 1a - 1c. Three slices from the central region of the imaging range were utilized for evaluation. For the acquired images, we designated regions of interest (ROIs) at three locations on each side of the spherical phantom, and we measured the signal values in air (Fig. 2). These measurements were subsequently compared, and statistical analysis was conducted utilizing the Kruskal-Wallis and Steel-Dwass multiple comparison tests (p < 0.05) (EZR v. 1.67 Jichi Medical University Saitama Medical Center, Saitama, Japan).

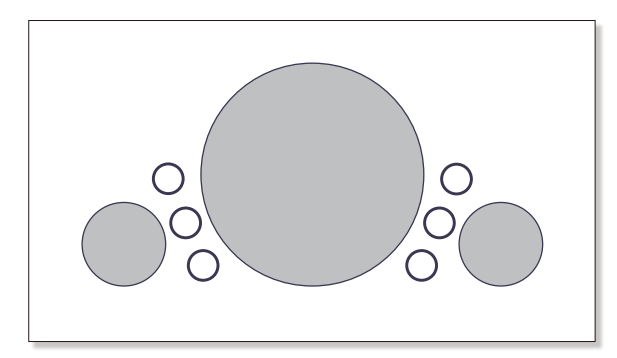


Fig. 2 ROI setting method for the measurement of signal intensity in air.

## Image uniformity

The phantom was imaged utilizing GRASP-VIBE and conventional VIBE in the seven configurations illustrated in Fig. 1a - 1g, and gray scale uniformity maps 10) were generated using the image of a single slice at the imaging center. Gray scale uniformity maps were created in accordance with the National Electrical Manufacturers Association (NEMA) method. A ROI at the center of the image was selected to encompass 75% of the signalproducing volume. The signal from each pixel in the entire image was examined, and a fivestep gray level was assigned to each pixel according to the magnitude by which the signal deviated from the mean value at the center ROI. A five-step gray-level representation of image nonuniformity was employed with the following ranges relative to the mean value:

A. lowest signal value to -20%

B. -20% through -10%

C. -10% through +10%

D. +10% through +20%

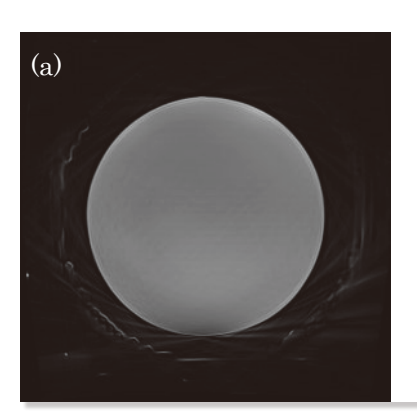
E. +20% through to highest signal value

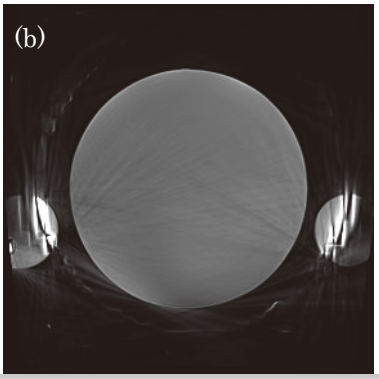
This map serves as a visual evaluation method for assessing the location and structure of nonuniformities but does not provide a quantitative value. Consequently, we obtained the percent image uniformity (PIU) from the gray scale uniformity map, referencing previous reports <sup>11)</sup> to compare the differences in phantom configuration and imaging sequence. The groups A - E aforementioned, designated for the creation of the gray scale uniformity map, were consolidated to form three distinct groups, 0 - 2:

Group 0: Total number of pixels from group C

Group 1: Total number of pixels from groups B and D

Group 2: Total number of pixels from groups A and E





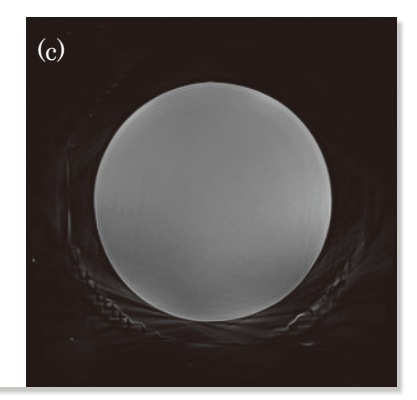


Fig. 3 Phantom image by GRASP-VIBE.

- (a) Phantom configuration A
- (b) Phantom configuration B
- (c) Phantom configuration C

The number of pixels in each of these groups was then used to compute a PIU as follows:

PIU = 
$$100 (1 - (0.5 \cdot \text{group1} + \text{group2}) / (\text{group0} + \text{group1} + \text{group2})) \dots (1)$$

# Results

### Streaking artifacts

Images obtained from the three distinct phantom configurations utilized for evaluation, along with graphs generated from the measured data, are presented in Figs 3 and 4. The median values for configurations A, B, and C were 45.52, 104.52, and 60.63, respectively. A Kruskal-Wallis test revealed a significant difference among the three configurations (p < 0.05). Post-hoc multiple comparisons using the Steel-Dwass test indicated significant differences between configuration A and B (p < 0.05), as well as between configuration B and C (p < 0.05). However, no significant difference was found between configuration A and C (p = 0.63).

# Image uniformity

Gray scale uniformity maps obtained through GRASP-VIBE and conventional VIBE imaging techniques are presented in Figs 5 and 6. In conventional VIBE imaging, phantom configurations C, E, and G displayed

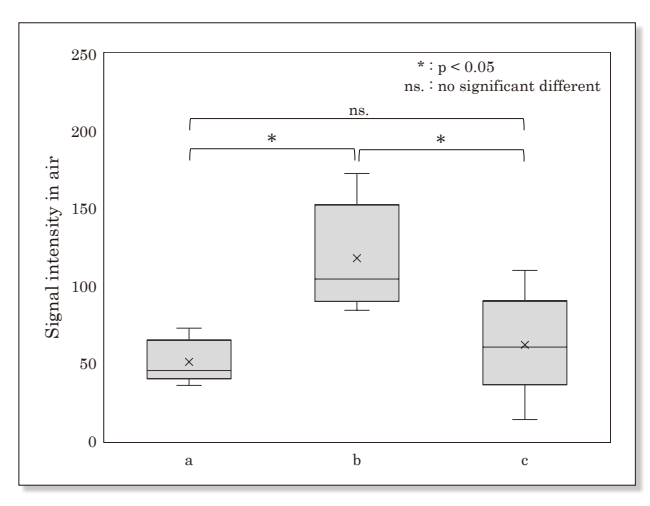


Fig. 4 Measured signal value in air to evaluate streaking artifacts.

- (a) Phantom configuration A
- (b) Phantom configuration B
- (c) Phantom configuration C

heightened signals near the sheet within the spherical phantom. However, in GRASP-VIBE, phantom configuration C showed lower signal values within the spherical phantom between EWS sheets, while phantom configurations E and G exhibited reduced signal values in the anterior region of the spherical phantom. PIUs for seven distinct phantom arrangements obtained via GRASP-VIBE and conventional VIBE are enumerated in Table 1. Comparing identical phantom placements with and without the EWS sheet encircling the cylindrical phantom revealed that GRASP-VIBE showed a reduction of 11.26% to 14.09%

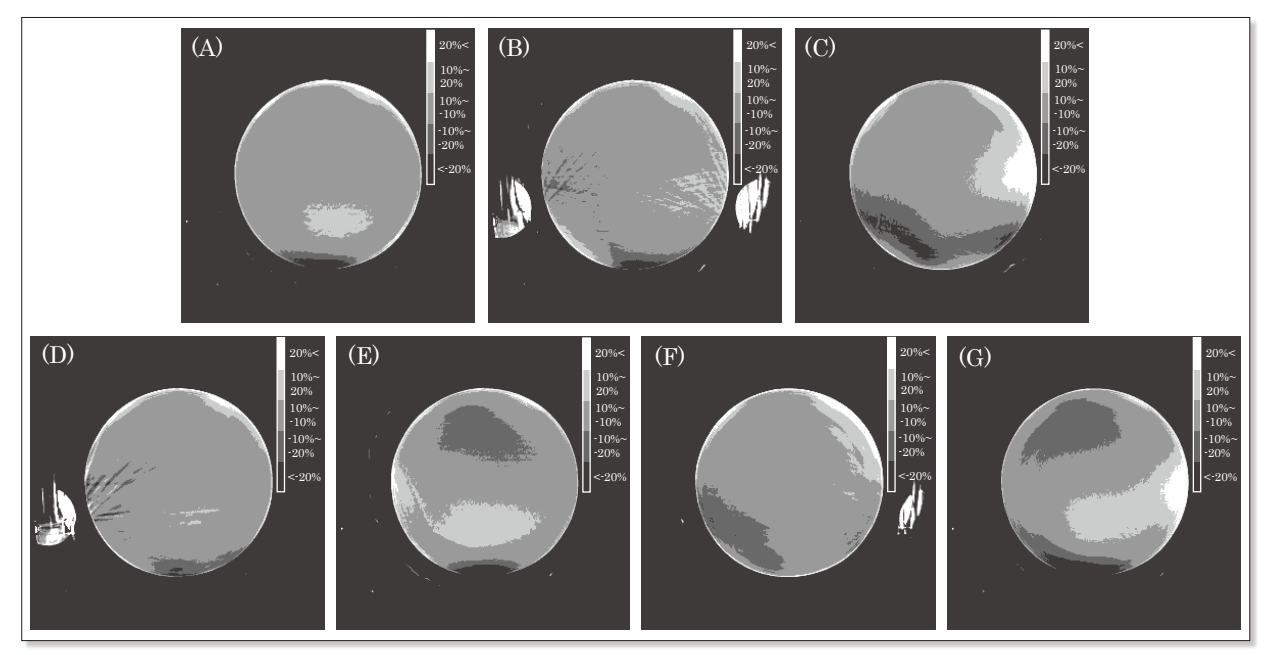


Fig. 5 Gray scale uniformity map of GRASP-VIBE in 7 different phantom configurations.

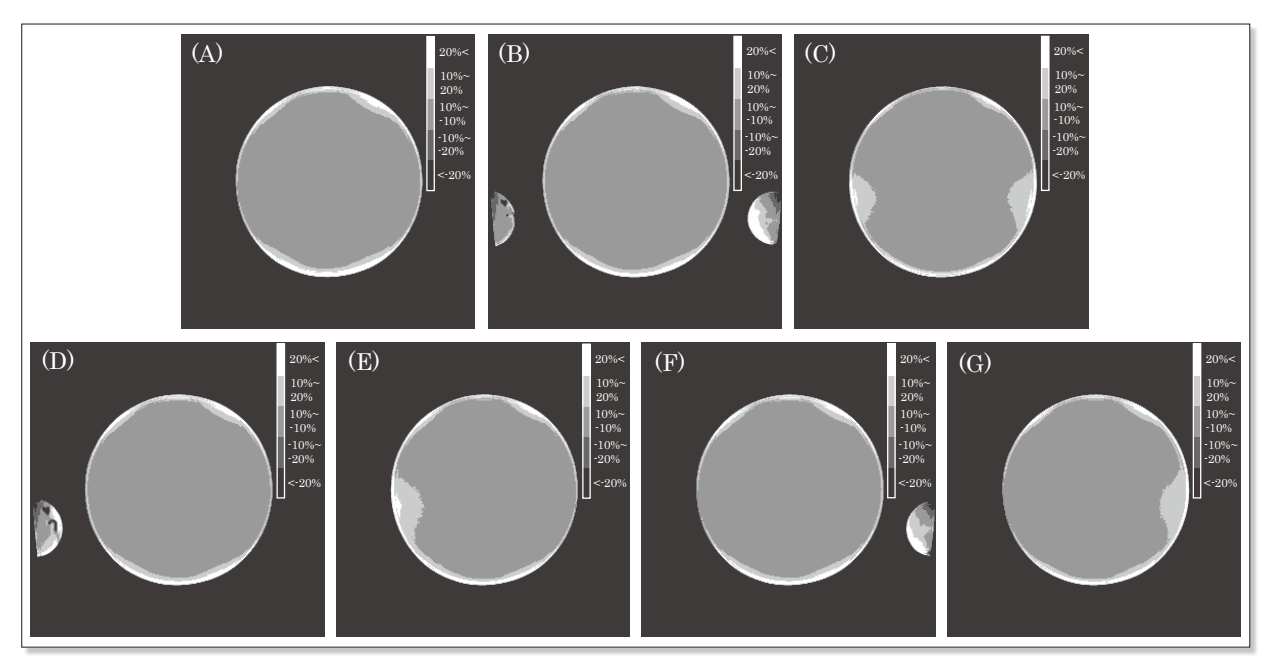


Fig. 6 Gray scale uniformity map of conventional VIBE in 7 different phantom configurations.

Table 1 The percent image uniformities for GRASP-VIBE and conventional VIBE at each phantom configuration.

Percent image uniformity							
Phantom configuration	А	В	С	D	Е	F	G
GRASP-VIBE	88.14	87.41	73.32	89.67	78.41	84.08	70.85
Conventional VIBE	90.55	91.52	89.30	91.22	89.38	91.38	89.72

in PIUs when the EWS sheet was applied, compared to when it was not used. On the other hand, conventional VIBE showed a decrease of 1.66% to 2.22%.

# Discussion

In this investigation, we evaluated the influence of wrapping the EWS sheet around the arm on images acquired during upper abdominal imaging with GRASP-VIBE, using a phantom. The EWS sheet demonstrated efficacy in mitigating streaking artifacts caused by the arm. Nonetheless, its placement was observed to potentially result in a reduction of signal intensity in the abdominal region, thereby affecting the overall uniformity of the image.

GRASP-VIBE incorporates fat suppression techniques; however, when the arm is drooped, adequate fat suppression is often not achieved, particularly in off-center regions where the arm is positioned, due to the nonlinearity of the magnetic field gradient. As a result, streaking artifacts arising from the arm that maintain high signal values are generated, thereby deteriorating the image quality of the abdomen. Our experimental findings indicated that the presence of cylindrical phantoms exacerbated streaking artifacts, as evidenced by differences in signal values in air with and without these phantoms. We hypothesized that wrapping EWS sheets around cylindrical phantoms, the primary source of streaking artifacts, suppressed signal values, thus mitigating the artifacts. Validation results demonstrated that the utilization of EWS sheets significantly mitigated streaking artifacts. Nevertheless, the utilization of EWS sheets resulted in signal irregularities within the spherical phantom, with numerous artifacts emerging from high-signal regions on the phantom's bedside surface. The artifact induced a slight increase in the background signal value; however, there was no statistically

significant difference compared to the scenario without the cylindrical phantom. Given that the streaking artifacts originating from the edges of the spherical phantom had minimal impact on its interior, it is anticipated that imaging with the EWS sheet encircling the patient's arm will effectively mitigate the artifacts.

To ensure image uniformity, seven distinct phantom configurations were employed, and an evaluation was conducted using a gray scale uniformity map in accordance with the NEMA method. This approach enabled the identification of areas exhibiting signal irregularities. To facilitate numerical comparisons, PIU values were calculated based on the grayscale uniformity map and referenced prior studies. The noticeable decrease in PIU was more pronounced with GRASP-VIBE compared to conventional VIBE, a phenomenon that can be attributed to the radial acquisition scheme used in GRASP-VIBE. Radial acquisitions allow for continuous sampling of the k-space center and provide robustness against motion artifacts. However, the presence of phase errors in k-space data can negatively impact image quality 12, 13). These errors can be caused by echo shift resulting from inhomogeneities in the static magnetic field and imbalances in the imaging gradients, which are mainly caused by eddy currents. The EWS sheet utilized in this study comprises copper and carbon, both of which are conductive materials. Upon exposure to electromagnetic waves, conductors generate electric currents due to the force acting on free electrons. These currents manifest as eddy currents, creating a magnetic field around the conductor 14). This magnetic field, in turn, induces static magnetic field inhomogeneity, leading to echo shift and subsequent phase errors, resulting in trajectory errors in k-space and variations in signal intensity in images. For the above reasons, the reduction in uniformity observed when utilizing the EWS sheet during GRASP-VIBE imaging is hypothesized to be attributable to eddy currents generated in the EWS sheet upon exposure to electromagnetic waves. In Cartesian acquisitions, such as conventional VIBE, rectilinear k-space undergoes uniform shifts and uniform phase errors across all lines 14). Consequently, Cartesian acquisitions are less likely to degrade image quality due to phase errors. Changes in signal intensity in Cartesian acquisitions are likely attributed to the influence of the non-uniform RF magnetic field caused by RF waves reflected by the sheet and are confined to the vicinity of the sheet. Furthermore, in radial acquisitions, the disturbance of the static magnetic field by eddy currents varies based on the sheet's position, exerting different effects on the image. The use of EWS sheets on only one side of the cylindrical phantom exacerbates PIU reduction and image quality degradation. Therefore, when utilizing GRASP-VIBE with EWS sheets, it is recommended to wrap EWS sheets around both arms to prevent a decline in image quality.

This study employed a phantom commonly used for MRI system maintenance. Although the experiments were conducted with a setup designed to simulate the human body, the shape and signal characteristics differ from those of actual biological tissue. Furthermore, in clinical settings, variations in subject body size and intra-abdominal tissue composition may result in differences in signal disturbances and their spatial manifestations. Subsequent validation utilizing volunteer studies and clinical data is imperative in future research. Additionally, this study was conducted under imaging conditions relevant to clinical settings, and images were evaluated following sensitivity correction processing. In 3T MRI systems, multi-channel coils are utilized, and sensitivity correction holds significant importance in clinical practice. However, the impact on images is expected to vary depending on the coils used and the distance from the specimen.

# Conclusion

The application of an EWS sheet to cover the dependent arms during GRASP-VIBE imaging may potentially mitigate streaking artifacts in upper abdominal imaging. This approach could potentially enhance image quality at the lateral margins of abdominal organs in proximity to the arms. However, due to radial sampling, static magnetic field inhomogeneity induced by the EWS sheet may result in signal intensity variations within the FOV. Notably, the utilization of the sheet on a single arm may adversely affect image uniformity, thus rendering the application of sheets to both arms preferable. Furthermore, signal attenuation between the two sheets may potentially lead to image quality degradation. Consequently, prudence is warranted when employing this technique for examinations focusing on abdominal organs in the posterior region.

# Disclosure Statement

The authors declare that they have no conflicts of interest.

# 表の説明

Table 1 GRASP-VIBEと従来のVIBEの各ファントム配置における画像均一性の割合.

### 図の説明

Fig.1 7つのファントムの模式図.

(A) 中央の球状ファントム. (B) 球形ファントムの両側に配置された円筒形ファントム. (C) 円筒ファントムにシートを巻いた配置B. (D) 球状ファントムの右側のみに円柱ファントムを配置したもの. (E) 円筒ファントムの周りにシートを巻いた配置D. (F) 球状ファントムの左側のみに円筒ファントムを配置したもの. (G) 円柱ファントムの周りにシートを巻いた配置F.

Fig.2 空気中の信号値測定のためのROI設定位置。

Fig.3 GRASP-VIBEによるファントム画像

- (a) ファントム配置 A
- (b) ファントム配置 B
- (c) ファントム配置 C

- Fig.4 ストリークアーチファクト評価用の信号値.
  - (a) ファントム配置 A
  - (b) ファントム配置 B
  - (c) ファントム配置 C
- Fig.5 GRASP-VIBEで取得した7種類の異なるファントム配置でのグレイスケールマップ.
- Fig.6 従来のVIBEで取得した7種類の異なるファントム配置 でのグレイスケールマップ.

### References

- Feng L, et al.: Golden-angle radial sparse parallel MRI: combination of compressed sensing, parallel imaging, and golden-angle radial sampling for fast and flexible dynamic volumetric MRI. Magn Reson Med, 72(3), 707-717, 2014.
- Pan J, et al.: Image quality optimization: dynamic contrast-enhanced MRI of the abdomen at 3T using a continuously acquired radial golden-angle compressed sensing acquisition. Abdom Radiol (NY), 49, 399-405, 2024.
- Lu Y, et al.: The value of GRASP on DCE-MRI for assessing response to neoadjuvant chemotherapy in patients with esophageal cancer. BMC Cancer, 19(1), 999, 2019.
- Xue Y, et al.: Automatic coil selection for streak artifact reduction in radial MRI. Magn Reson Med, 67(2), 470-476, 2012.
- Du J, et al.: Artifact reduction in undersampled projection reconstruction MRI of the peripheral vessels using selective excitation. Magn Reson Med, 51(5), 1071-1076, 2004.

- Mandava S, et al.: Radial streak artifact reduction using phased array beamforming. Magn Reson Med, 81(6), 3915-3923, 2019.
- Ono A, et al.: Effect of electromagnetic wave suppression sheet in magnetic resonance imaging system on radio-frequency-induced heating of metallic implant. JJMRM, 39(2), 55-59, 2019.
- Ministry of Health, Labor and Welfare: Report of National Health and Nutrition Survey in Japan, 2019. Ministry of Health, Labor and Welfare, 122-123, 2020.
- Ito K, et al.: Non-contrast MR angiography of the renal artery with golden angle radial sparse parallelvolumetric interpolated breath-hold examination: Optimal imaging conditions. JJMRM, 43(4), 174-181, 2023.
- 10) National Electrical Manufacturers Association: Determination of image uniformity in diagnostic magnetic resonance images. NEMA Standards Publication MS 3-2008.
- 11) Goerner FL, et al.: A comparison of five standard methods for evaluating image intensity uniformity in partially parallel imaging MRI. Med Phys, 40(8), 082302, 2013.
- Moussavi A, et al.: Imperfect magnetic field gradients in radial k-space encoding-Quantification, correction, and parameter dependency. Magn Reson Med, 81(2), 962-975, 2019.
- 13) Moussavi A, et al.: Correction of gradient-induced phase errors in radial MRI. Magn Reson Med, 71(1), 308-312, 2014.
- 14) Hidaka K.: Introduction to Materials Designing for Electromagnetic Wave Shielding or Absorption. Seikei-Kakou, 34(1), 5-8, 2022.